Joint Pathology Center

Veterinary Pathology Services

WEDNESDAY SLIDE CONFERENCE 2016-2017

C o n f e r e n c e 16

25 January 2017

CASE I: AR-14-1021 (JPC 4066394).

Signalment: Eight-month-old, Dorset ewe, (*Ovis aries*).

History: This ewe was enrolled in a research study in which it underwent surgery and MRI the following day, both under general anesthesia. The ewe initially recovered normally, displaying brief weakness in the hindlimbs immediately after surgery. However, over the next two weeks, it gradually became dull and lethargic, dehydrated, inappetent, and weakened despite supportive care. The animal was found recumbent, hypothermic, tachycardic, and dyspneic 13 days after surgery and died before it was able to be euthanized.

Gross Pathology: The major gross lesion was in the lungs. The right cranial lung lobe was half normal size, mottled dark red to black, and firm on palpation. The cranial aspect of the right middle lung lobe appeared similarly. Dissection of the bronchial tree did not reveal the presence of foreign material. Additionally, several ulcers, up to 1 x 2 cm, were present in the trachea.

Gross Morphologic Diagnosis: Broncho-pneumonia, multifocal, subacute, severe, necrotizing.

Laboratory results: Bacterial culture of the lung yielded a pure culture of *Trueperella pyogenes.*

Histopathologic Description: The lung is markedly hypercellular, owing to filling of alveoli by degenerate inflammatory cells, amorphous and fibrillar eosinophilic material (edema and fibrin, respectively), basophilic streaming nuclear and eosinophilic cytoplasmic debris, and myriad gram-positive bacterial rods. In some regions, well-defined areas with architectural preservation without cellular

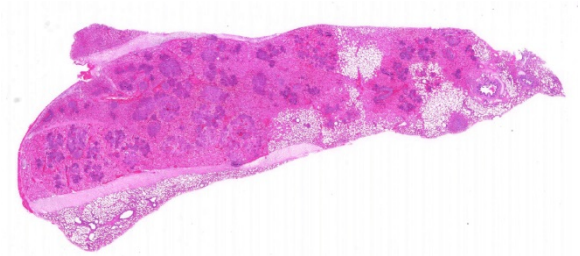

Lung, ewe. At subgross magnification – there is diffuse severe alveolar edema and hemorrhage, marked intraseptal edema, and numerous well-demarcated areas of cellular infiltrate and necrosis. (HE, 5X)

detail (coagulative necrosis) are present. Bronchi and bronchiole lumina frequently contain abundant bacteria and sloughed bronchial epithelium. Interlobular septa are thickened up to 2mm wide by fibrin and edema, and blood vessels were congested and contained bacteria. The pleura is expanded up to 3x normal with blood.

Contributor's Morphologic Diagnoses: Bronchopneumonia, diffuse, subacute, severe, necrotizing, with myriad gram-positive bacteria.

Contributor's Comment: All findings in this case were consistent with bronchopneumonia caused by *Trueperella pyogenes* (formerly *Arcanobacterium pyogenes),* a gram-positive non-motile, non-sporeforming, short, rod-shaped bacterium.[6] *Trueperella pyogenes* is one of the most common opportunistic pathogens in domestic livestock and is often commensal flora in the mammary gland, upper respiratory, urogenital, and gastrointestinal tracts.[6,10] Although *T. pyogenes* can act as a primary pulmonary pathogen, infection usually follows physical or microbial trauma which overcomes the pulmonary defense mechanisms, allowing for colonization of the lungs.[1,8] The pneumonia was initially suspected to be due to aspiration shortly after recovery from anesthesia, but foodstuff was not present in the respiratory tract. The reason for the infection was likely due to a combination of stressors, including what was interpreted as intubation-associated ulceration of the trachea.

Trueperella pyogenes produces and utilizes a variety of virulence factors to colonize, damage, and persist within a variety of tissues in the host. The most important factor is pyolysin (PLO), a cytolysin, which is able to bind to and create pores in the cell membranes of erythrocytes,

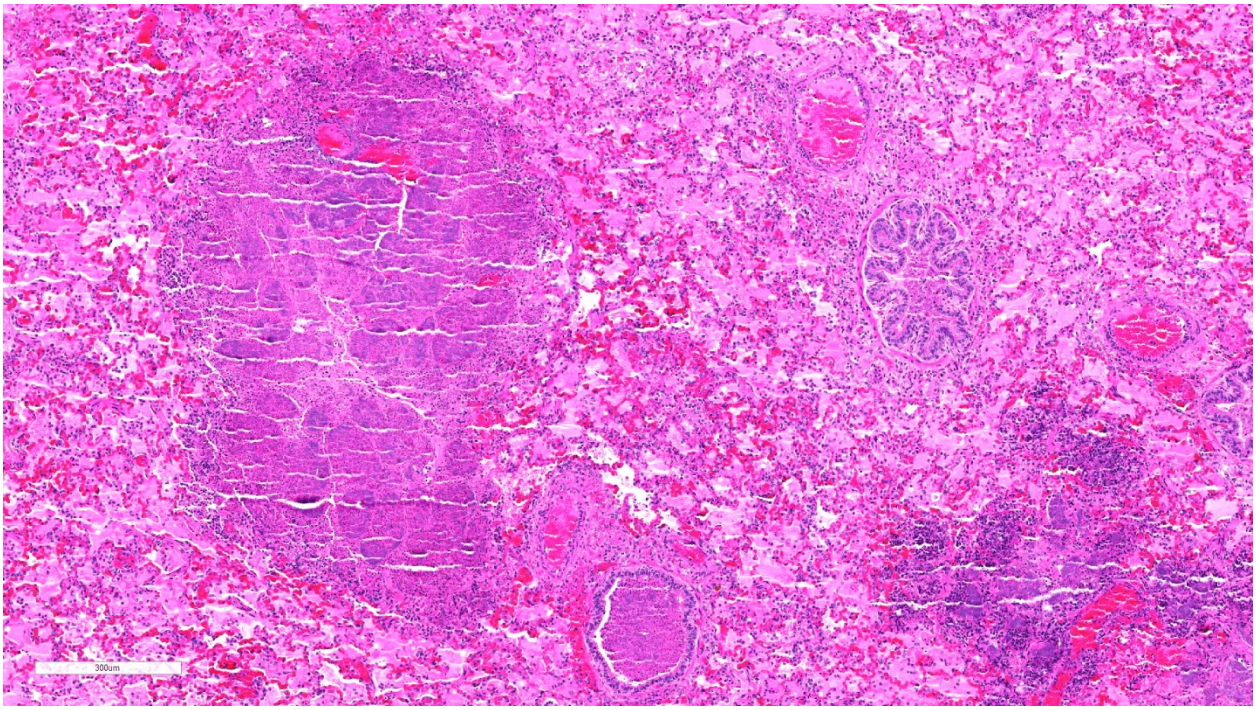

Lung, ewe. Multifocally airways and alveoli contain varying combinations and concentrations of necrotic debris, large colonies of bacilli, edema, and hemorrhage. (HE, 88X)

polymorphonuclear cells, and macrophages resulting in cell lysis.[6] *Trueperella pyogenes* mutants lacking the PLO gene were unable to cause an intraperitoneal infection in mice injected with 10^8 bacteria, whereas replacement of the PLO gene to the *T. pyogenes* mutants restored full virulence.[5] Additional virulence factors used by *T. pyogenes* include fimbriae[13], extracellular matrix binding proteins specific for collagen[4], fibrinogen, fibronectin[5], and exoenzymes including DNases[11], proteases[12], and neuraminidases[7] which degrade host nucleic acids, proteins, and sialic acid residues, respectively.

Note: Multiple different tissue sections of lung were used for the slides submission; therefore, not all the participants will receive similar serial microslide sections.

JPC Diagnosis: Lung: Bronchopneumonia, necrotizing and fibrinosuppurative, multifocal to coalescing, severe, with marked alveolar and septal edema and numerous large colonies of bacilli, Dorset sheep, *Ovis aries*.

Conference Comment: This case demonstrates the characteristic gross and histologic lesions associated with bacterial bronchopneumonia. Conference participants described the suppurative inflammation filling bronchi and bronchioles surrounded by multifocal to coalescing areas of necrosis, and readily identified numerous large colonies of bacilli within the areas of inflammation. Participants discussed the differential diagnosis for large colony forming bacteria in tissue section to include: *Yersinia* sp, *Actinomyces* sp., *Actinobacillus* sp., *Corynebacterium* sp, *Staphylococcus* sp., *Streptococcus* sp., and *T. pyogenes*. *Trueperella pyogenes* is one of the most common opportunistic pathogens present on the mucosal surfaces of domestic animals.[1,2,5,8] The bacterium induces suppurative inflammation within a wide

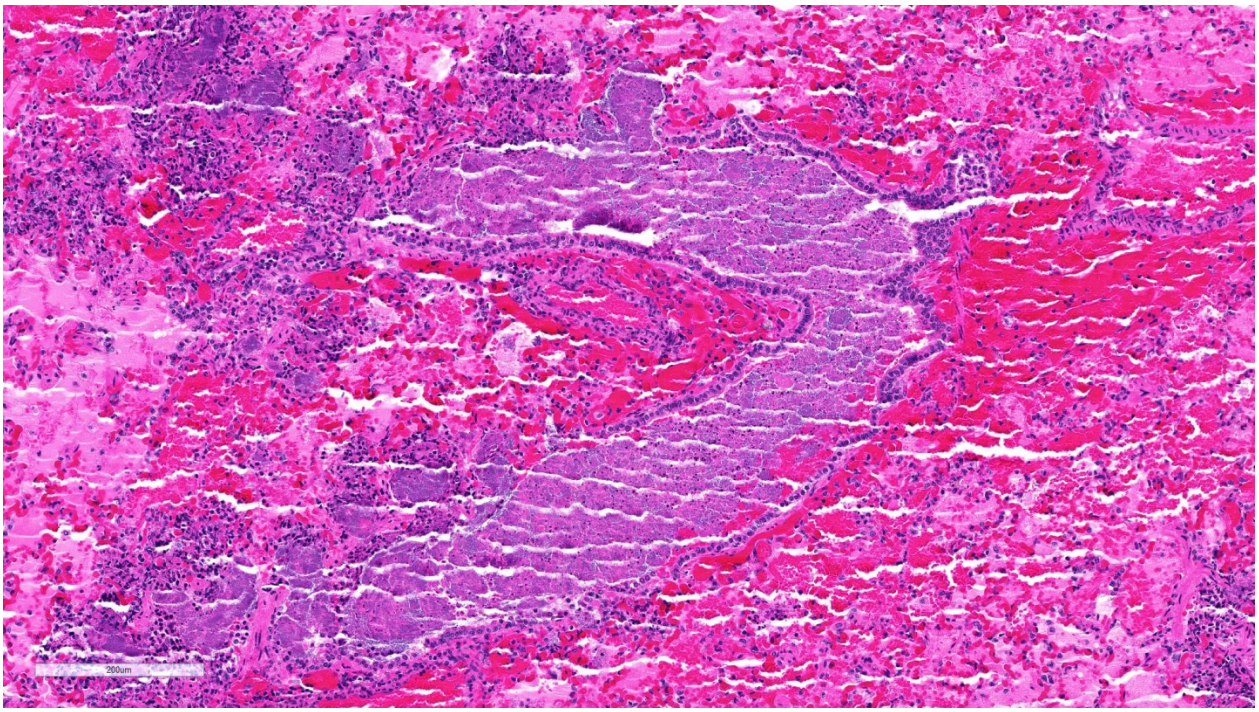

Lung, ewe. There is extensive involvement of airways and necrosis is primarily relegated to the adjacent alveoli, suggesting an aerogenous entry for the causative agent. (HE, 96X)

variety of organs and is an important cause of abortion, arthritis, endocarditis, mastitis, osteomyelitis, and pneumonia resulting in significant losses in production animals.[2,4] Additionally, *T. pyogenes* is widespread in the wild animal population and has been reported as an important cause of cerebral abscesses in young male white-tailed deer as a consequence of antler development and conspecific aggression between bucks. Mortality can reach up to 35% in affected free-ranging adult male deer.[3]

As mentioned by the contributor, while *T. pyogenes* can be a primary pathogen, it is usually associated with physiologic trauma to a mucosal membrane, concurrent primary infection, or immune suppression.[1,2,3,8] As postulated by the contributor in this case, there well may be an association with placement of the endotracheal tube. Other common commensal organisms of the ruminant upper respiratory tract that can cause opportunistic bronchopneumonia include *Mannheimia haemolyica*, *Pasteurella multocida*, and *Bibersteinia trehalosi*. Causes of primary infectious pneumonia in sheep include parainfluenza virus 3, respiratory syncytial virus, and *Bordetella parapertussis*, which can predispose sheep to secondary infection by the commensal bacteria mentioned above.[1,3,8] *Mycoplasma ovipneumoniae* is another important primary etiologic agent involved in chronic enzootic pneumonia; also known as chronic non-progressive pneumonia, it is a multi-factorial disease complex affecting lambs less than one-year-old. *Mycoplasma ovipneumoniae* usually causes a mild, subclinical infection that results in poor growth unless complicated by stressors such as over-crowding, inclement weather, or poor air quality.[1,2,3,8]

Another primary cause of pneumonia in sheep includes the maedi-visna virus, which

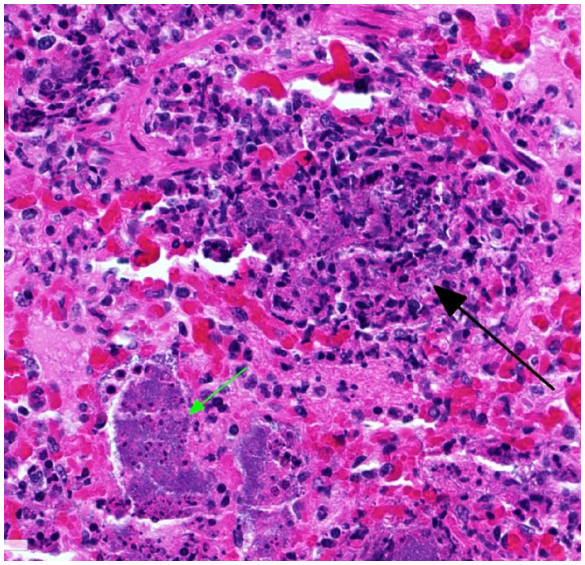

Lung, ewe. Alveoli are filled with a combination of degenerate epithelium and heterophils with streaming nuclear material (consistent with "oat cells") (black arrow) and large colonies of bacilli predominate in some alveoli (green arrow.)

results in lifelong persistent viral infection and leads to ovine progressive pneumonia (OPP), encephalitis, arthritis, and mastitis in sheep. This lentivirus is a member of the family *Retroviridae*, and is closely related to caprine arthritis-encephalitis virus. First reported in Iceland, the "maedi" (respiratory form) occurs in sheep older than three years, while the "visna" (neurologic form) occurs in younger sheep.[1,9] The respiratory form is characterized by interstitial pneumonia with prominent perivascular and peribronchial lymphoid nodules. This slowly progressive pneumonia is often complicated by secondary bacterial infection, especially *T. pyogenes*.[1] Peste des petits ruminants (PPRV), a morbillivirus, has also been reported to cause primary respiratory disease in small ruminants in Africa and parts of Asia. This virus primarily affects the cranioventral lung lobes and causes a bronchointerstitial pneumonia.[1,8,9]

Contributing Institution:
Wake Forest School of Medicine

Department of Pathology/Comparative Medicine
Medical Center Boulevard
Winston Salem, NC 27157-1040
http://www.wakehealth.edu/Comparative-Medicine/

References:

1. Caswell JL, Williams KJ. Respiratory system. In: Maxie MG, ed. *Jubb, Kennedy, and Palmers Pathology of Domestic Animals*. 6th ed. Vol. 2. Philadelphia, PA: Elsevier; 2016:557-560.
2. Cohen BS, Belser EH, et al. Isolation and genotypic characterization of *Trueperella* (*Arcanobacterium*) *pyogenes* recovered from active cranial abscess infections of male white-tailed deer (Odocoileus virginianus). *J Zoo Wildl Med*. 2015; 46(1):62-67.
3. Dassanayake RP, Shanthalingam S, Herndon CN, et al. *Mycoplasma ovipneumoniae* can predispose bighorn sheep to fatal *Mannheimia haemolytica*pneumonia. *Vet Microbiol*. 2010; 145:354-359.
4. Esmay PA, et al. The *Arcano-bacterium pyogenes* collagen-binding protein, CbpA, promotes adhesion to host cells. *Infect Immun*. 2003; 71(8):4368-74.
5. Jost BH, Billington SJ. *Arcano-bacterium pyogenes*: Molecular pathogenesis of an animal opportunist. *Antonie Van Leeuwenhoek*. 2005; 88(2):87-102.
6. Jost BH, Songer JG, Billington SJ. An *Arcanobacterium (Actinomyces) pyogenes* mutant deficient in production of the pore-forming cytolysin pyolysin has reduced virulence. *Infect Immun*. 1999; 67(4):1723-8.
7. Jost BH, Songer JG, Billington SJ. Cloning, expression, and characterization of a neuraminidase gene from *Arcanobacterium pyogenes*. *Infect Immun*. 2001; 69(7):4430-7.
8. Lopez A, Martinson SA. Respiratory system, mediastinum, and pleurae. In: *Pathologic Basis of Veterinary Disease*. Zachary JM ed. 6th ed. St. Louis: Elsevier; 2017:537-540.
9. MacLachlan NJ, Dubovi EJ, eds. *Fenners Veterinary Virology*. 4th ed. London, UK: Elsevier; 2011:267-268,308-323.
10. Queen C, Ward AC, Hunter DL. Bacteria isolated from nasal and tonsillar samples of clinically healthy Rocky Mountain bighorn and domestic sheep. *J Wildl Dis*. 1994; 30(1):1-7.
11. Ramos, CP, Foster G, Collins MD. Phylogenetic analysis of the genus Actinomyces based on 16S rRNA gene sequences: description of *Arcanobacterium phocae* sp. nov., *Arcanobacterium bernardiae* comb. nov., and *Arcanobacterium pyogenes* comb. nov. *Int J Syst Bacteriol*, 1997; 47(1):46-53.
12. Takeuchi S, Kaidoh T, Azuma R, Assay of proteases from *Actinomyces pyogenes* isolated from pigs and cows by zymography. *J Vet Med Sci*. 1995; 57(5):977-9.
13. Yanagawa R, Honda E Presence of pili in species of human and animal parasites and pathogens of the genus *Corynebacterium*. *Infect Immun*. 1976; 13(4):1293-5.

CASE II: Case 2 (JPC 4085015).

Signalment: Six-month-old, male, Tonkinese cat, (*Felis catus*).

History: The cat presented for further investigation of a vestibular ataxia, head tremors, inappetence, and lethargy. The cat was in poor body condition compared to its littermate and had previously been found to be pyrexic. Neurological examination findings were consistent with a central vestibular syndrome. MRI of the brain revealed marked dilatation of the third and fourth ventricles and mild dilatation of the lateral ventricles. There was marked contrast enhancement of the ependymal lining and meninges, consistent with feline infectious peritonitis and obstructive hydrocephalus. Cerebellar herniation was present with caudal displacement of the cerebellar vermis through the foramen magnum, consistent with elevated intracranial pressure. A provisional diagnosis of feline infectious peritonitis (FIP) was made. Due to a grave prognosis, the cat was euthanized and submitted for necropsy examination.

Gross Pathology: An increased volume of clear fluid drained from the cranium as the brain was removed and there appeared to be diffuse flattening of the cortical gyri. The brain was dissected following fixation and there was moderate dilation of the third, fourth and lateral ventricles.

Laboratory results: Feline coronavirus antibody titer was extremely high; CSF (post mortem) showed a marked, mixed pleocytosis with neutrophilic predominance and markedly increased protein concentration.

Histopathologic Description: Brain: Sections of forebrain, midbrain, cerebellum and brainstem are examined. Variably within the examined sections the meninges, choroid plexus and ependyma are multifocally and extensively expanded by dense infiltrates of lymphocytes, plasma cells, macrophages and rare viable and degenerate neutrophils. There is prominent perivascular cuffing, predominantly targeting veins, of periventricular and meningeal blood vessels by lymphocytes, macrophages, plasma cells and occasional viable and degenerate neutrophils. The inflammatory infiltrate extends into both vascular walls and beyond the Virchow-Robin spaces into the adjacent neuropil. There is a mild to moderate gliosis within the adjacent neuropil and periventricular white matter contains variably-sized extracellular clear spaces (edema). Ependymal cells lining the ventricles appear mildly elongate with disruption and increased spacing between cells.

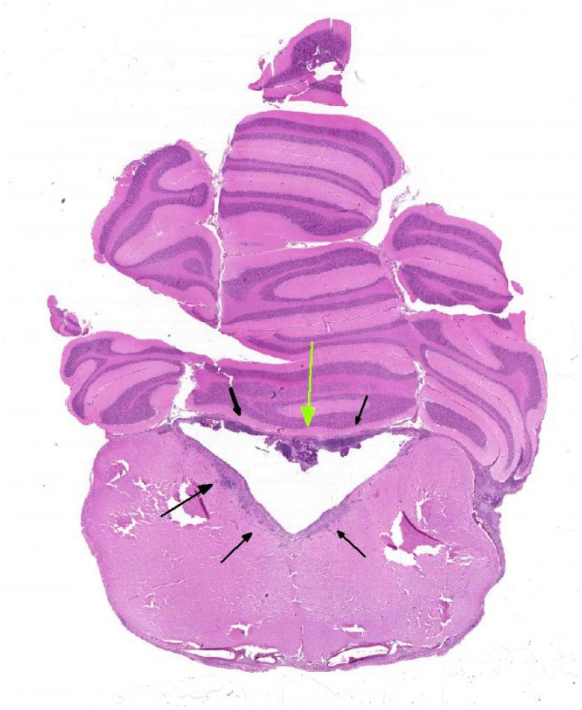

Cat, fourth ventricle. There is marked hypercellularity surrounding the 4th ventricle and brainstem meninges (black arrow), as well as expansion of the choroid plexus (green arrow.) (HE, 5X)

Multifocally, there is necrosis of the ventricular lining with deposition of fibrin.

Immunohistochemistry:
Immunohistochemical labeling for feline coronavirus antigen identified scattered, large, foamy round cells (macrophages) which labeled positively for Coronavirus antigen within the lesions in the brain tissue.

Contributor's Morphologic Diagnoses: 1. Brain: multifocal, marked, pyo-granulomatous and lymphoplasmacytic meningoencephalitis with vasculitis and perivasculitis, ventriculitis, choroiditis and ependymitis
2. Brain: moderate acquired hydrocephalus

Contributor's Comment: Feline coronaviruses (FCoVs) are enveloped, single-stranded, positive-sense RNA viruses that belong to the *Coronaviridae* family, *Alphacoronavirus* genus and exist as two pathotypes, feline infectious peritonitis virus (FIPV) and feline enteric coronavirus (FECV).[1,3] Despite FCoVs being ubiquitous in the environment, with a prevalence of more than 90% of cats in multicat households, feline infectious peritonitis (FIP) is sporadic, with young, entire male, purebreed cats most commonly affected[1]. Feline enteric coronavirus is generally considered avirulent, however, can be associated with hemorrhagic enteritis and diarrhoea[3] and affected cats may become persistently infected and continue to shed virus. In contrast, FIPV results in severe, systemic disease and is a common cause of neurologic disorders in young cats.[2]

Feline coronavirus is generally transmitted via the fecal-oral route following which it infects enterocytes, eventually being restricted to the caecum and colon.[1] Analysis of FECVs and FIPVs suggests a

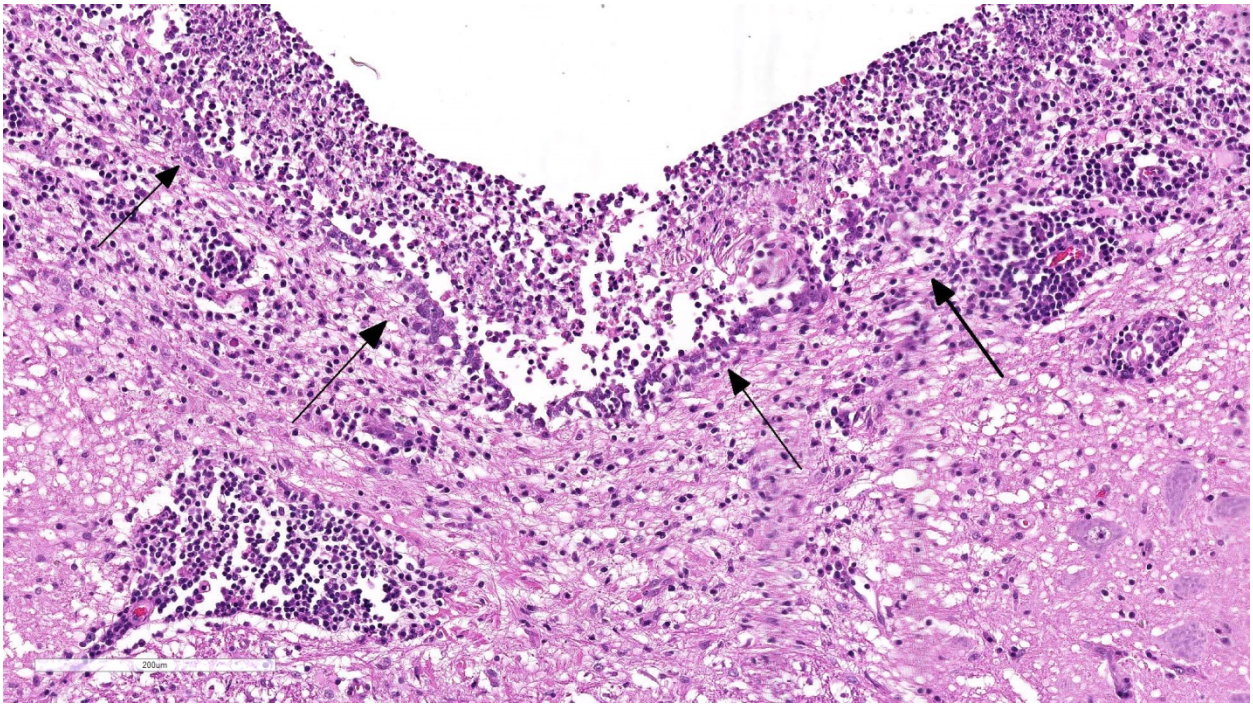

Cat, fourth ventricle and underlying brainstem. The lumen of the fourth ventricle contains numerous degenerate neutrophils and macrophages, admixed with polymerized fibrin and cellular debris. The ependyma (black arrows) is multifocally ulcerated. Brainstem vessels are surrounded by large numbers of lymphocytes and plasma cells. (HE, 196X)

complex scenario involving several gene mutations to result in increased virulence[1,3]. Feline infectious peritonitis viruses appear to have an increased ability to replicate in macrophages and monocytes and result in systemic disease.[1] Virus-infected macrophages localize to small and medium sized veins within the serosa and damage endothelial cells with the subsequent immune response resulting in a vasculitis. A strong cell-mediated response is protective against FIP, whereas a weak cell-mediated response results in the 'dry' form of the disease. The 'wet' form of disease results from a lack of cell-mediated immune response to the virus. Both type III and type IV hypersensitivity responses have been implicated in the pathogenesis of FIP.[5]

Feline infectious peritonitis is often distinguished by a 'wet' or effusive form and a 'dry' non-effusive form with a proportion of cases showing a combination of the two. Typical gross findings associated with the effusive form of FIP include a fibrinous and granulomatous peritonitis, protein rich effusions and visceral granulomatous inflammatory foci. In 60% of non-effusive cases of FIP there is involvement of the eyes and/or CNS with or without granulomatous lesions in the thoracic and abdominal viscera and frequently in the absence of a grossly apparent peritonitis[2]. Gross lesions in the brain are often unapparent, however may include thickening and opacity of the meninges, and an obstructive hydrocephalus, as seen in this case. Proteinaceous material within the ventricular system may be visible as grey-blue gelatinous material.[4] Clinical signs associated with FIP are often vague and include pyrexia, lethargy and inappetence with additional changes dependent on the distribution of tissues affected.[2]

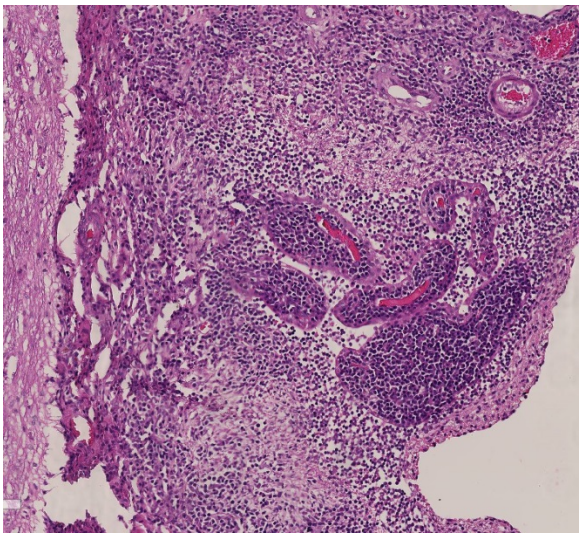

Cat, brainstem meninges: The meninges are expanded by large numbers of macrophages, lymphocytes and plasma cells. Lymphocytes and plasma cells have a marked perivascular distribution. (HE, 100X)

The characteristic microscopic findings associated with FIP include a vasculitis and perivasculitis, predominantly affecting small to medium sized venules.[3] A high proportion of macrophages alongside variable numbers of neutrophils, lymphocytes and plasma cells infiltrate and surround vessels. Vascular necrosis with thrombosis and infarction may also occur.[2] Feline infectious peritonitis may be suspected based on the signalment, compatible clinical signs, and identification of pathognomonic gross and histologic lesions. Identification of viral antigen in lesions using immunohistochemistry or real time RT-PCR is confirmatory for a diagnosis of FIP.[3]

JPC Diagnosis: Cerebrum, brainstem: Meningoencephalitis, lymphoplasmacytic and histiocytic, perivascular, diffuse, moderate to marked with lymphoplasmacytic and histiocytic choroiditis and phlebitis, Tonkinese cat, *Felis catus*.

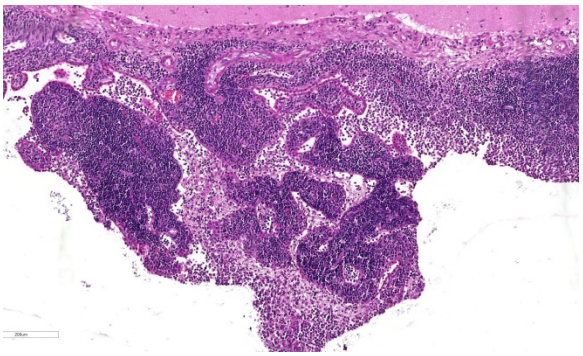

Cat, choroid plexus, fourth ventricle. The vascular bed of the choroid plexus is also markedly expanded by numerous lymphocytes and plasma cells. (HE, 100X)

Conference Comment: Although there is some moderate slide variability, we thank the contributor for providing an excellent example and review of feline infectious peritonitis (FIP), a disease that is caused by a mutated feline enteric coronavirus (mutated FCoV). Given the history provided by the contributor, this case is likely more consistent with the non-effusive form of FIP with lesions restricted to the central nervous system, although the distinction between the wet and dry form is somewhat arbitrary and the disease likely represents a continuum rather than two distinct clinical forms.[3] As mentioned by the contributor, neurologic signs due to encephalitis or meningitis are present in approximately 60% of all FIP cases.[4,5] Chronic ventriculitis, choroiditis, and ependymitis causes outflow obstruction of the cerebrospinal fluid from the ventricular system of the brain leading to marked dilation of the ventricles.[5] This dilation of the ventricles leads to a compression atrophy of the proximate neuroparenchyma because of the lack of expansibility within the skull. The resulting increased intracranial pressure then results in both hydrocephalus and caudal displacement and herniation of the cerebellum through the foramen magnum, present in this case. FIP remains as one of the most common causes of infectious death in cats with Bengals, Birmans, Himalayans, ragdolls, and Rexes significantly overrepresented for the development of the disease.[3]

A recent publication in *Veterinary Pathology* by Kiper and Meli[1] outlined three key features as prerequisites for the development of FIP: a) systemic infection with virulent mutated FCoV, b) effective viral replication in circulating monocytes, and c) activation of mutated FCoV-infected monocytes.[1] Although avirulent FCoV is readily transmitted via the fecal-oral route, most believe that the mutated virulent form is not transmitted horizontally, but is rather the result of spontaneous mutation within each cat that develops FIP. The hallmark lesion of FIP is granulomatous or lymphohistiocytic phlebitis, present in this case, which is mediated by activated

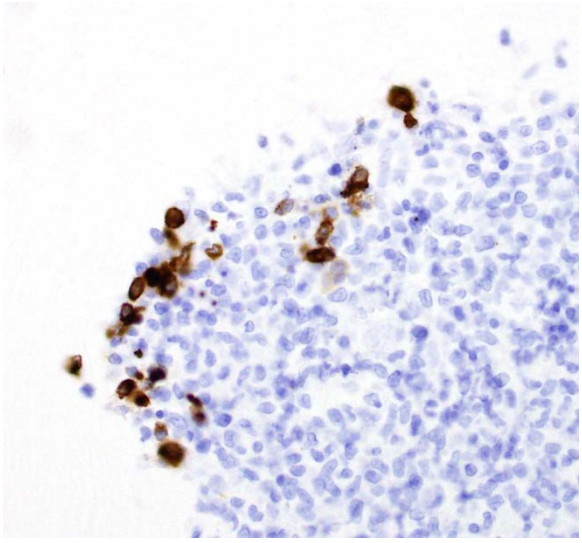

Cat, fourth ventricle: Macrophages within these areas multifocally exhibited strong cytoplasmic labeling for coronaviral antigen. (400X)

circulating monocytes during viremia. Activated monocytes upregulate adhesion molecules such as CD18, and produce pro-inflammatory cytokines such as TNF-α, IL-1b, GM-CSF, and IL-6, in addition to matrix metalloproteinases (MMP-9), and vascular endothelial growth factor (VEGF). Endothelial cells appear to be selectively responsive and activated by the cytokine

storm generated, which limits the distribution of lesions to veins within select organs. The trigger for the massive monocyte activation and selectivity of lesion location is not currently known.[1]

Conference participants discussed the nature of the immune response by the host as a determining factor for which form of the disease the animal will have. As mentioned by the contributor, mutated FCoV-infected circulating monocytes are likely responsible for viremia. The conference moderator instructed that cats with a strong cell-mediated immune (CMI) response do not develop FIP.[1,3,5] Alternative, a weak CMI and strong humoral response results in the effusive, or wet form of the disease. This form is characterized by vasculitis, peritonitis and profound thoracic and peritoneal effusion as a result of deposition of antigen-antibody complexes (type III hypersensitivity).[3,5] In addition, these cats are hypergammaglobulinemic due to the overproduction of ineffective antibodies. In contrast, the noneffusive dry form of the disease is associated with a moderate CMI response with pyogranulomatous inflammation (type IV hypersensitivity) and develop clinical signs based on the organs affected, such as the brain in this case. However, as noted above, the different forms represent a continuum and most cases are likely a mix of the two extreme forms of the disease.[1,3,5]

Contributing Institution:
Dept. of Pathology and Pathogen Biology
Royal Veterinary College, London, UK
http://www.rvc.ac.uk/pathology-and-diagnostic-laboratories

References:

1. Kipar A, Meli ML. Feline infectious peritonitis: still an enigma? *Vet Pathol*. 2014; 51(2)**:**505-526.
2. Pedersen NC: A review of feline infectious peritonitis virus infection: 1963-2008. *J Feline Med Surg*. 2009; 11(4)**:**225-258.
3. Uzal FA, Plattner BL, Hostetter JM. Alimentary System. In: Maxie MG, ed. *Jubb, Kennedy and Palmer's Pathology of Domestic Animals*. Vol 2. 6th ed. Missouri: Elsevier; 2016:253-254.
4. Vandevelde M, Higgins RJ, Oevermann A. *Veterinary Neuropathology: Essentials of Theory and Practice*. Oxford: Wiley-Blackwell; 2012.
5. Zachary J, McGavin M. Nervous system. In: *Pathologic Basis of Veterinary Disease*. 5th ed. Missouri: Elsevier; 2012:860-861.

CASE III: 15-008432 (JPC 409).

Signalment: Two-year-old, male, spayed female, beagle (*Canis familiaris*).

History: The dog presented for chylothorax after lobectomy at a referral surgical center several months before. After surgery, there was a persistent effusion that was managed with an indwelling Pleura-Port. The dog received a short course of cyclosporine for the effusion. On recheck, there was a significant decline in clinical condition (not really consistent with a cylothorax). Radiographs at that time showed the development of a diffuse milliary pattern not reported on original films or seen at rDVM a few weeks earlier. Based on the report, cyclosporine was discontinued and the dog was sent to the rDVM (owner's relative) to consider options. The plan was for the patient to return for lung biopsy in a few days but the dog continued to decline and after a night on oxygen with minimal

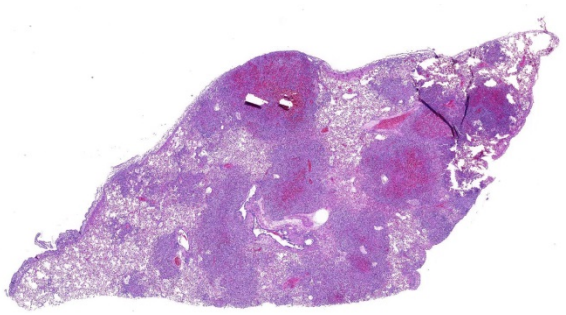

Lung, dog. The submitted sections contains numerous well-defined areas of hypercellularity which efface underlying parenchyma. (HE, 5X).

stabilization and much less improvement, euthanasia was performed. Only lung tissue was submitted by the clinician for histopathology.

Gross Pathology: Sections of formalin-fixed lung were mottled tan-red on cut section.

Laboratory results: N/A

Histopathologic Description: Lung: There are extensive multifocal to coalescing areas of tissue necrosis admixed with hemorrhage, fibrin, edema, karyorrhectic and occasionally mineralized debris; these areas are variably centered on partially or fully effaced bronchioles. Within these foci are florid infiltrates of viable and degenerate neutrophils, large foamy macrophages, and multinucleated macrophages, as well as myriad amoebic trophozoites and rare cysts. Trophozoites are 25-30-um in diameter, with flocculent pale eosinophilic cytoplasm and a 6-8-um karyosome with a prominent central basophilic endosome. Cysts measure 15-20-um and have a thick, bilayered wall (exocyst and endocyst). Within the nucleus of macrophages (including multinucleated macrophages phagocytizing trophozoites) adjacent to and within the most severely affected regions of the lung, there are one to multiple prominent brightly eosinophilic intranuclear inclusions that peripheralize the chromatin. In areas of the lung that are less severely affected, there is filling of alveolar spaces with edema, foamy macrophages, and low numbers of neutrophils, as well as scattered type II pneumocyte hyperplasia, hypertrophy of vascular endothelial cells, and expansion of residual septa by fibrin, similar inflammatory cells, and hyper-trophied fibroblasts. There is mild multifocal mesothelial hypertrophy.

Immunohistochemistry for canine distemper virus was negative. In-situ hybridization with a probe directed against canine herpesvirus was also negative. Indirect immunofluorescence at the CDC confirmed the amoebae to be *Acanthamoeba* spp.

Contributor's Morphologic Diagnoses: Lung: Pneumonia and bronchiolitis, necrosuppurative and hemorrhagic, multi-focal, chronic-active, severe, with free and intrahistiocytic *Acanthamoeba* spp. trophozoites and cysts.

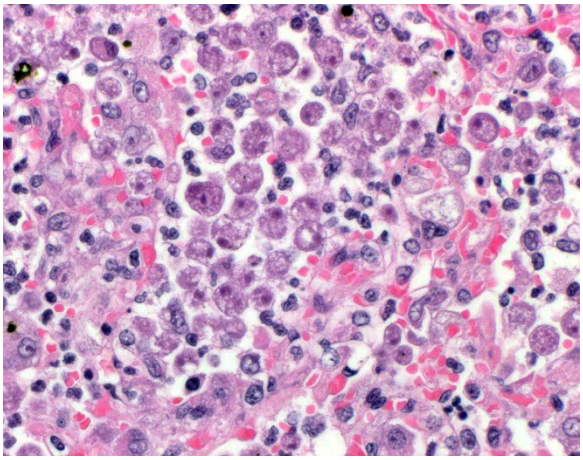

Lung, dog. Numerous Acanthamoeba trophozoites are present within the remnants of a bronchiole, as well as within the surrounding alveoli. (HE, 100X) (Photo courtesy of: Auburn University College of Veternary Medicine, Dept. of Pathobiology , 166 Greene Hall, College of Veterinary Medicine, Auburn University, Auburn, AL 36849).

Contributor's Comment: *Entamoeba histolytica, Sappinia diploidea, Acanthamoeba, Balamuthia* and *Naegleria* species are free-living amoebas that act as secondary decomposers and regulate bacterial population in the soil. However, they are also opportunistic pathogens and can cause severe disseminated disease or necrotizing granulomatous encephalitis in immunosuppressed animals and humans. In the present case, the patient had received a short course of cyclosporine to treat the pleural effusion, which was potentially responsible for the immune suppression and increased susceptibility to opportunistic pathogens. Due to the presence of both cysts and trophozoites in the lung tissues, infection with *Acanthamoeba spp.* or *Balamuthia mandrillaris* was suspected.[18] *Naegleria fowleri* is only present as trophozoites and does not form cysts in infected tissues.[18] However, a definitive diagnosis of *Acanthamoeba* infection was based on the positive results of indirect immunofluorescence.

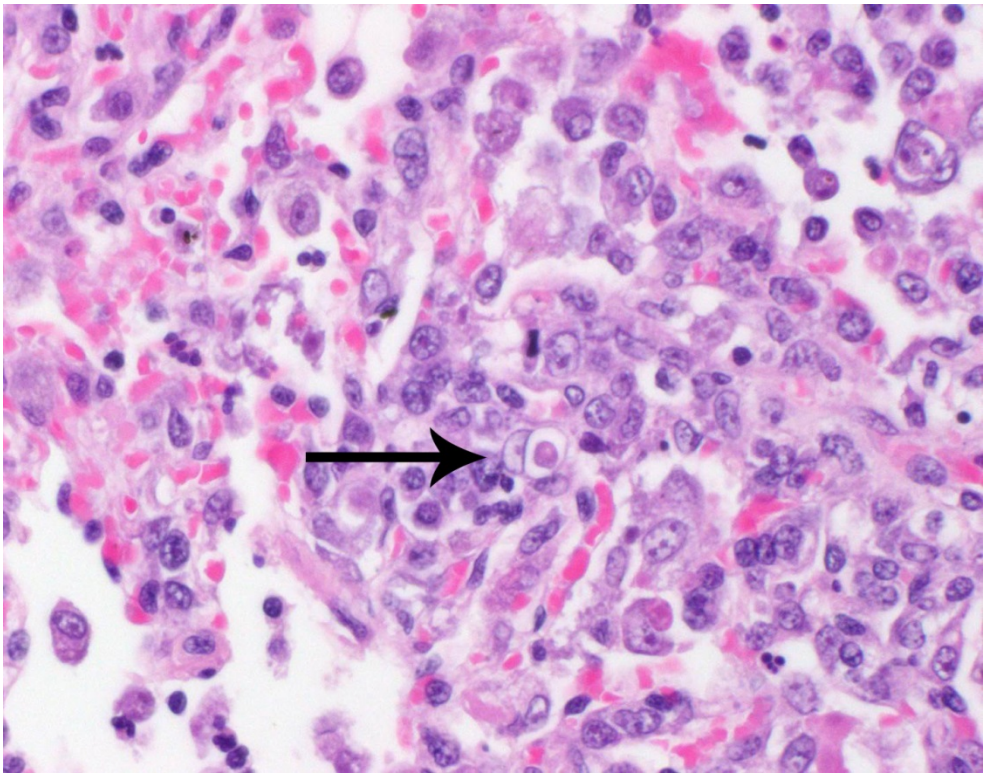

Lung, dog. Acanthamoeba cyst in the lung parenchyma that has a clear space between the exocyst and endocyst (arrow). (HE, 400X) (Photo courtesy of: Auburn University College of Veterinary Medicine, Dept. of Pathobiology, 166 Greene Hall, College of Veterinary Medicine, Auburn University, Auburn, AL 36849).

Acanthamoeba is ubiquitously present in the environment and has been isolated from diverse sources including sea water, beaches, pond water, soil, fresh water lakes, and even from the air. In human populations, anti-*Acanthamoeba* antibodies are present in up to 100% of people in healthy populations in New Zealand and in more than 85% of individuals of London who came from different countries.[3,5,18] In dogs, pulmonary infections usually result from inhalation or aspiration of the organisms from the water.

Acanthamoeba binds to host cells by a 130 kDa mannose-binding protein (MBP). *Other adhesions involved in this interaction include* laminin-binding protein with a predicted molecular mass of a 28.2 kDa, a 55 kDa laminin-binding protein and a > 207 kDa adhesion.[8,9,17] *Acanthamoeba* binding to the host cells results in its phagocytosis and release of toxins. Two superoxide dismutases, an iron superoxide dismutase and a copper-zinc superoxide dismutase

provide antioxidant defense. Toxins produced by *Acanthamoeba* cause activation of the phosphatidylinositol 3-kinase (PI3K) pathway, which further activates pro-apoptotic molecules, Bak and Bax, resulting in loss of mitochondrial membrane potential and apoptosis of host cells.[1,13,19] In host cells, toll-like receptor-4 (TLR4) is responsible for recognition of *Acanthamoeba*, which leads to activation of the Myd88 pathway and induces secretion of interleukin-8, tumor necrosis factor-alpha, and interferon-beta.[13,16] *Acanthamoeba* causes degradation of occludin and zonula occludens-1 tight junction proteins in human brain microvascular endothelial cells (HBMEC) in a Rho kinase-dependent manner, and thus leading to increased vascular permeability.[12]

Acanthamoeba causes cutaneous lesions, sinus infections, keratitis, and rare but fatal encephalitis, known as granulomatous amoebic encephalitis in humans. Similarly, *Acanthamoeba* causes encephalitis and disseminated disease in immunosuppressed animals. In addition, most isolates harbor endosymbionts including numerous viruses (vesicular stomatitis virus, adenovirus, and poliovirus), bacterias (*Burkholderia spp., Campylobacter jejuni, Coxiella burnetii, Francisella tularensis, Helicobacter pylori and Listeria monocytogenes*), and yeast organisms (*Cryptococcus neoformans, Blastomyces dermatitidis, Sporothrix schenckii, Histoplasma capsulatum*). However, the role of endosymbionts is not entirely clear. It is suspected that *Acanthamoeba* can transmit them to susceptible hosts or endosymbionts can increase the pathogenicity of *Acanthamoeba*.[11,18]

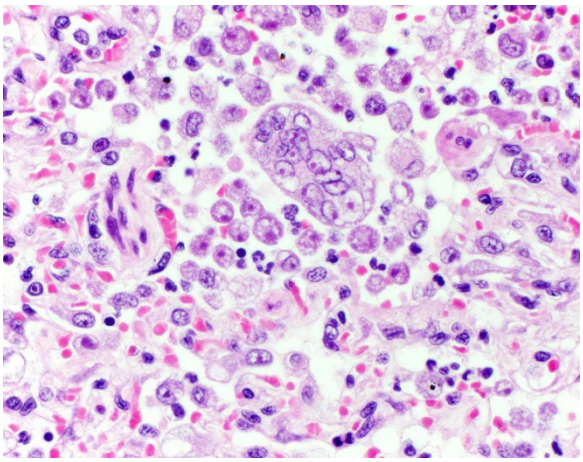

Lung, dog. Multifocally, alveolar spaces and discohesive lung parenchyma contained multinucleated giant cells with presumed intranuclear eosinophilic inclusion bodies. (HE, 400X) (Photo courtesy of: Auburn University College of Veterinary Medicine, Dept. of Pathobiology, 166 Greene Hall, College of Veterinary Medicine, Auburn University, Auburn, AL 36849).

The intrahistiocytic intranuclear inclusions present in this case are strongly suggestive of a co-infection with canine distemper virus. Unfortunately, the formalin-fixed tissue was held by the submitting clinician for several weeks prior to submission, so it is likely that this resulted in a loss of immunoreactivity due to antigen cross-linking.

JPC Diagnosis: Pneumonia, broncho-interstitial and necrotizing, multifocal to coalescing, marked, with free and intrahistiocytic trophozoites and rare cysts, beagle, *Canis familiaris*.

Conference Comment: We thank the contributor for providing an outstanding and challenging case that stimulated a great deal of discussion among the conference participants regarding whether *Acanthamoeba* is the primary cause of the significant pulmonary pathology in this case, or if it is secondary to concurrent infection with canine distemper virus (CDV). Like the contributor, many participants note numerous brightly eosinophilic intra-histiocytic nuclear inclusion bodies within multinucleated cells, which are interpreted as viral syncytial cells. However, others argue that the intranuclear structures may be

representative of prominent nucleoli in response to marked chronic inflammation and the multinucleated cells are reactive fused macrophages and megakaryocytes rather than viral syncytial cells. Participants also describe multinucleated cells that occasionally contain phagocytosed amoebic trophozoites.

bronchiolar epithelium do not contain prominent cytoplasmic inclusions typical of CDV. Unfortunately, as mentioned by the contributor, suboptimal tissue preservation techniques may have affected the immunoreactivity for canine morbillivirus immunohistochemistry (IHC). Additionally, formalin fixation dramatically reduces the

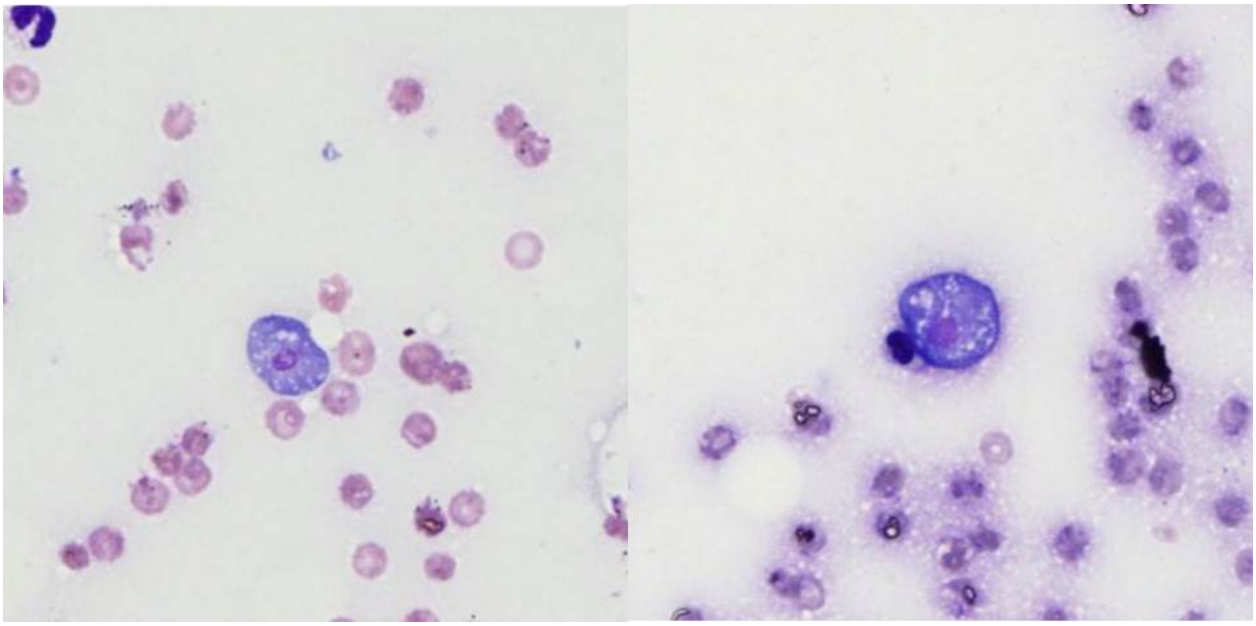

Lung, dog. Acanthamoeba trophozoites in lung aspirates stained with modified Wright's stain. (Wrights, 200X) (Photo courtesy of: Auburn University College of Veterinary Medicine, Dept. of Pathobiology, 166 Greene Hall, College of Veterinary Medicine, Auburn University, Auburn, AL 36849).

Ionized calcium binding adaptor molecule 1 (Iba1) immunohistochemical stain, provided by the contributor, demonstrated strong intracytoplasmic immunoreactivity for the multinucleated cells, confirming their macrophage lineage. The typical respiratory lesions associated with CDV include bronchointerstitial pneumonia with prominent cytoplasmic inclusion bodies in the bronchial and bronchiolar epithelium, type II pneumocyte hyperplasia with alveolar cytoplasmic inclusions, and alveolar epithelial syncytial cells.[4] Participants favoring primary *Acanthamoeba* infection note that bronchial and

ability to extract suitable DNA for PCR based diagnostic tests. These deleterious effects of formalin on DNA are time and concentration dependent.[14] The majority of participants agree with the contributor that there is likely primary concurrent infection with canine distemper virus in this case, despite negative IHC results.

Reports of pulmonary and systemic disease caused by free-living amoebae in dogs are uncommon and are usually associated with immune suppression with the majority of reported cases associated with underlying disease (such as co-infection with CDV) or long-term immunosuppressive doses of

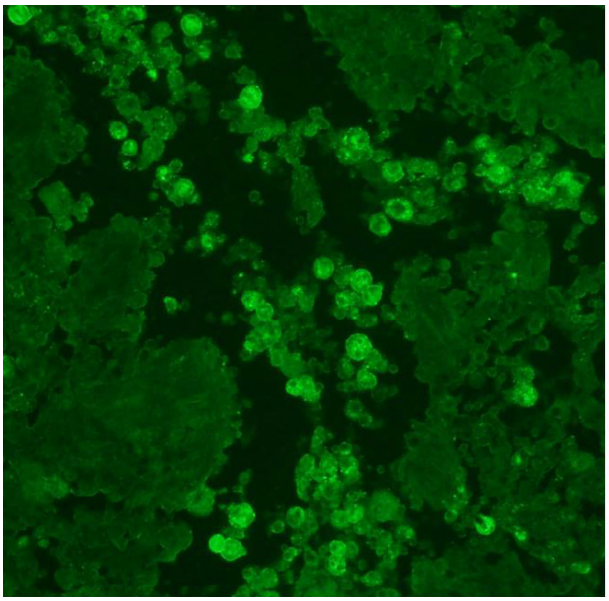
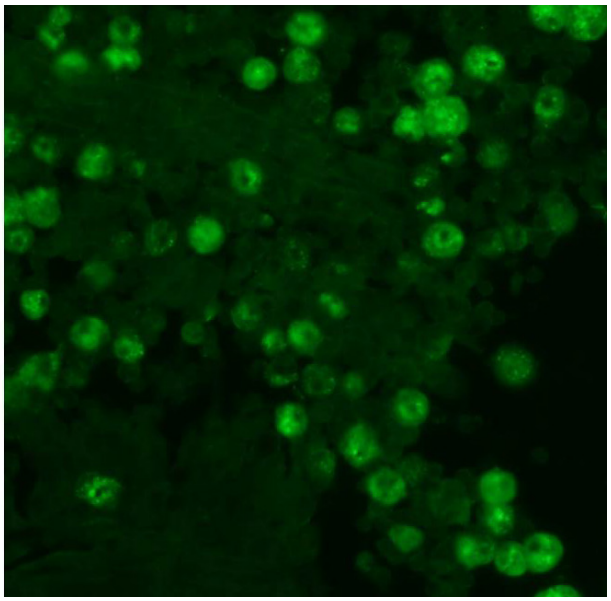

Lung, dog. Indirect immunofluorescence (IIF) assay on the lung tissue. In the IIF assay, 1:200 diluted rabbit anti-sera specific for Acanthamoeba species was used. Amoebae seen in the images ranged in size from 10-15 microns. (A) 200X magnification. (B) (Photo courtesy of: Auburn University College of Veterinary Medicine, Dept. of Pathobiology, 166 Greene Hall, College of Veterinary Medicine, Auburn University, Auburn, AL 36849).

corticosteroids[6,7,10,15]; however, there is a report of a greyhound naturally infected with *Acanthamoeba* sp. causing primary granulomatous pneumonia and encephalitis.[2] In this case, the dog was receiving cyclosporine to treat chylothorax after a lung lobectomy, which may offer an alternative explanation for immune suppression; however, the reported short course of treatment is inconsistent with the long course of immunosuppressive therapy reported in the literature.[6,7,1]

Contributing Institution:
Auburn University
College of Veterinary Medicine
Auburn, AL 36849
http://www.vetmed.auburn.edu/

References:

1. Alizadeh H, Pidherney MS, McCulley JP, Niederkorn JY. Apoptosis as a mechanism of cytolysis of tumor cells by a pathogenic free-living amoeba. *Infect Immun*. 1994; 62(4)**:**1298-1303.
2. Bauer R.W., Harrison L.R., Watson C.W., Styer E.L. & Chapman Jr W.L. 1993. Isolation of Acanthamoeba sp. from a greyhound with pneumonia and granulomatous amebic encephalitis. J. Vet. Diagn. Invest. 5:386-391.
3. Brindley N, Matin A, Khan NA. *Acanthamoeba castellanii*: High antibody prevalence in racially and ethnically diverse populations. *Exp Parasitol*. 2009; 121(3)**:**254-256.
4. Caswell JL, Williams KJ. Respiratory system. In: *Jubb Kennedy and Palmer's Pathology of Domestic Animals*. Vol 1. 6th ed. Philadelphia, PA: Elsevier Saunders; 2016:574-576.
5. Cursons RT, Brown TJ, Keys EA, Moriarty KM, Till D. Immunity to pathogenic free-living amoebae: Role of humoral antibody. *Infect Immun*. 1980; 29(2)**:**401-407.

6. Dubey JP, Benson JE, et al. Dissemninated *Acanthamoeba* sp. infection in a dog. *Vet Parasitol*. 2005; 125:183-187.
7. Foreman O, Sykes J, et al. Dissemniated infection with *Balamuthia mandrillaris* in a dog. *Vet Pathol*. 2004; 41:506-510.
8. Garate M, Cao Z, Bateman E, Panjwani N. Cloning and characterization of a novel mannose-binding protein of Acanthamoeba. *J Biol Chem*. 2004; 279(28)**:**29849-29856.
9. Hong YC, Lee WM, Kong HH, Jeong HJ, Chung DI. Molecular cloning and characterization of a cDNA encoding a laminin-binding protein (AhLBP) from Acanthamoeba healyi. *Exp Parasitol*. 2004; 106(3-4)**:**95-102.
10. Kent M, Platt S, et al. Multisystemic infection with Acanthamoeba sp in a dog. *J Am Vet Med Assoc*. 2011; 238:1476-1481.
11. Khan NA. Acanthamoeba: Biology and increasing importance in human health. *FEMS Microbiol Rev*. 2006; 30(4)**:**564-595.
12. Khan NA, Siddiqui R. Acanthamoeba affects the integrity of human brain microvascular endothelial cells and degrades the tight junction proteins. *Int J Parasitol*. 2009; 39(14)**:**1611-1616.
13. Mattana A, Cappai V, Alberti L, Serra C, Fiori PL, Cappuccinelli P. ADP and other metabolites released from *Acanthamoeba castellanii* lead to human monocytic cell death through apoptosis and stimulate the secretion of proinflammatory cytokines. *Infect Immun*. 2002; 70(8)**:**4424-4432.
14. Ramos F, Zurabian R, et al. The effect of formalin fixation on polymerase chain reaction characterization of *Entamoeba histolytica*. *Trans R Soc Trop Med Hyg*. 1999; 93:335-336.
15. Reed LT, Miller MA, Visvesvara GS, Gardiner CH, et al. Diagnostic exercise: Cerebral mass in a puppy with respiratory distress and progressive neurologic signs. *Vet Pathol*. 2010; 47(6):1116-1119.
16. Ren MY, Wu XY. Toll-like receptor 4 signalling pathway activation in a rat model of Acanthamoeba Keratitis. *Parasite Immunol*. 2011; 33(1)**:**25-33.
17. Rocha-Azevedo B, Jamerson M, Cabral GA, Marciano-Cabral F. *Acanthamoeba culbertsoni*: analysis of amoebic adhesion and invasion on extracellular matrix components collagen I and laminin-1. *Exp Parasitol*. 2010; 126(1)**:**79-84.
18. Siddiqui R, Khan NA. Biology and pathogenesis of Acanthamoeba. *Parasit Vectors*. 2012:5-6.
19. Sissons J, Kim KS, Stins M, Jayasekera S, Alsam S, Khan NA. *Acanthamoeba castellanii* induces host cell death via a phosphatidylinositol 3-kinase-dependent mechanism. *Infect Immun*. 2005; 73(5)**:**2704-2708.

CASE IV: 16-9986 (JPC 4084207).

Signalment: Seven-year-old quarter horse mare (*Equus ferus caballus*).

History: In June 2015, the horse presented to the referring veterinarian with bilateral conjunctivitis that progressed to severe anterior uveitis in the left eye. Foot abscesses, distal limb cellulitis, mandibular lymphadenopathy, nasal discharge, and hives developed subsequently. Treatments

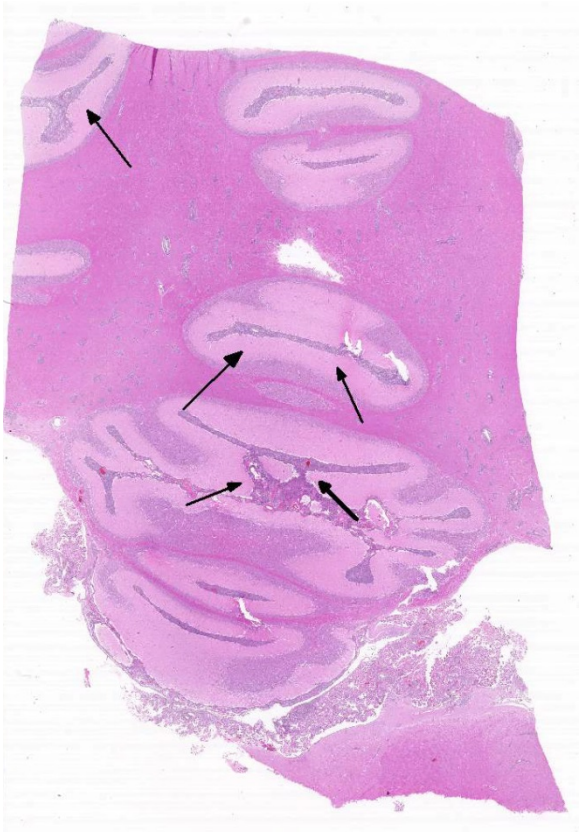

Cerebellar meninges, horse. Meninges are diffusely and markedly hypercellular and expanded. (HE, 5X)

included ceftiofur, oxytetracycline, dexamethasone, nonsteroidal anti-inflammatory drugs, and a two-week course of doxycycline. Despite treatment, the horse remained hyperfibrinogenemic at 800-1300 mg/dL and developed narcolepsy a few months later. Due to health concerns and the poor prognosis, the horse was euthanized in January 2016 and submitted to Cornell Animal Health Diagnostic Center for necropsy and tissue collection.

Gross Pathology: There was approximately 200 mL of yellow tinged transparent fluid (serous effusion) within the peritoneal cavity. The capsular surface of the liver was diffusely thickened, mottled white to tan to purple to black. There were thousands of multifocal to coalescing, generalized, white, 1-3 mm, hard white nodules along the capsular surface with a few dozen similar nodules within the parenchyma. Similar nodules were present in the thymus and surrounding the mediastinal fat and in all lung lobes. These nodules were presumed to be parasitic granulomas, which were confirmed histologically. Evidence of chronic laminitis was present in both forelimbs. The brain was grossly normal.

Laboratory results: Bloodwork in early December 2015 revealed elevated gamma glutamyl transferase (GGT) at 61 U/L (normal range 9-24 U/L), rising globulins at 2.3 g/dL from a previous value of 1.6 g/dL (normal range 2.8-4.7 g/dL), and a lymphocyte count of 1,940 cell/uL, up from a previous count of 1,380 cells/uL (normal range 1,000-4,900 cells/uL; lymphopenia is <1,500 cells/uL).

B cell concentration was markedly decreased at 19 cells/uL of 1,940 total lymphocytes/uL (0.98% B cells), with 1.0% CD19 B cells (median, CI = 9.0%, 2.0%), 0.2% CD21 B cells (median, CI = 10.2%, 4.2%), and 0.9% IgM B cells (median, CI = 10.2%, 2.1%).
The CD4+ and CD8+ T-cell distributions were slightly increased, and the CD4/CD8 ratio was within the normal reference interval.

Serum IgG concentration was markedly decreased at 423 mg/dL (median, CI = 1,760 mg/dL, 603 mg/dL) and serum IgM concentration was within the normal reference interval at 63 mg/dL (median, CI = 100 mg/dL, 50 mg/dL; deficiency is < 25 mg/dL).

Lyme titers on multiplex PCR assay (OspA, OspC, OspF) decreased from 2013 when they ranged 100-300 to June 2015, August 2015, and January 2016 when antibody titers were in the single digits and teens.

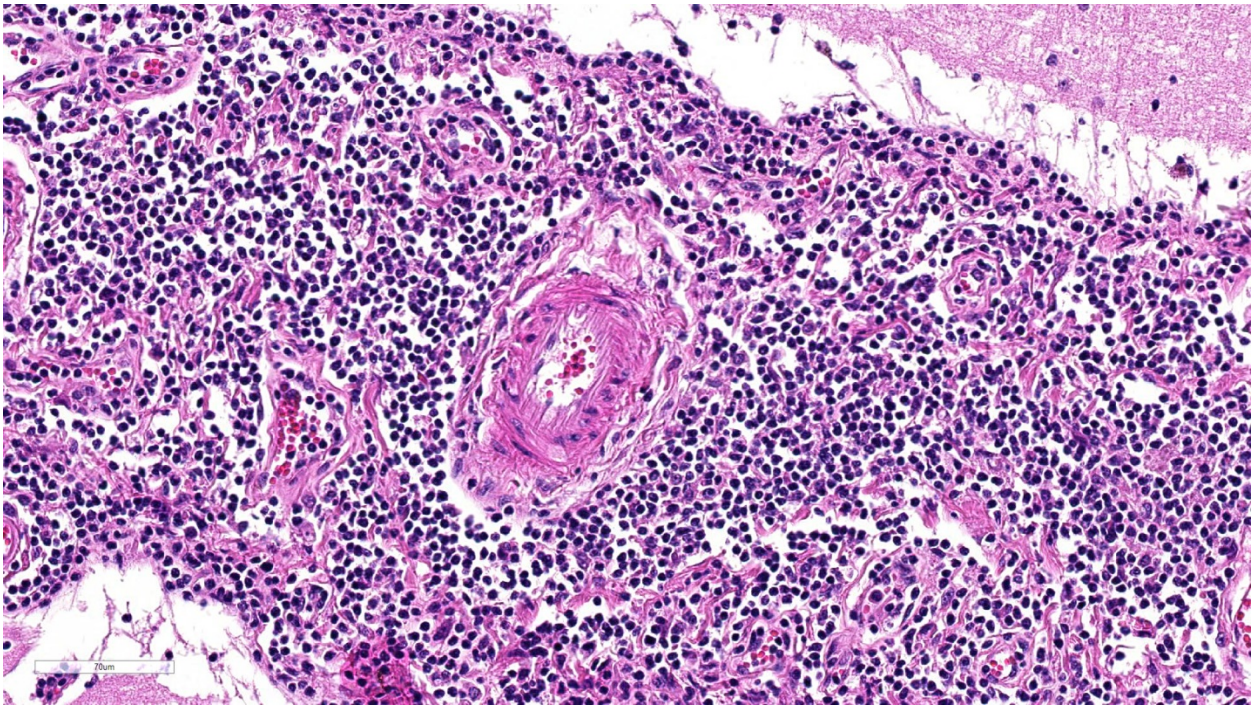

Cerebellar meninges, horse. Numerous lymphocytes and plasma cells with histiocytes and rare neutrophils expand the meninges. (HE, 164X)

Bacterial cultures and virus isolation of brain tissue were both negative. A quantitative PCR for *Borrelia burgdorferi* yielded a CT value of 32 (positive result).

Histopathologic Description: Brain, cerebrum, and cerebellum: Diffusely, meninges of the cerebellum and cerebrum are markedly expanded by a dense infiltrate of lymphocytes, macrophages, fewer neutrophils, and rare plasma cells interspersed with rare wispy spirochetal bacteria. Within the neuroparenchyma, the Virchow-Robin spaces of blood vessels are surrounded by a similar inflammatory infiltrate. Blood vessels are often prominent, characterized by endothelial hypertrophy and have variable branching. In the white and grey matters are increased numbers of enlarged glial cells with increased eosinophilic cytoplasm (astrocytes, presumptive). Multifocally within the choroid plexus are clusters of lymphocytes and histiocytes, along with few eosinophils.

Contributor's Morphologic Diagnoses: 1. Brain, cerebrum, and cerebellum: Severe, multifocal to coalescing, chronic lymphohistiocytic neutrophilic meningo-encephalitis with lymphohistiocytic eosinophilic choroid plexitis, branching blood vessels, astrocytosis, and rare intralesional spirochetal organisms

Other final morphologic diagnoses (slides not included):

2. Lymphohistoicytic meningo-myeloencephalitis and radiculoneuritis of the spinal cord and ganglia, respectively
3. Moderate, multifocal, chronic lymphocytic hypophysitis
4. Multifocal, chronic parasitic granulomas in the liver, lung, and thymus
5. Chronic lymphoplasmacytic portal hepatitis with capsular and bridging fibrosis
6. Multifocal laminitis and chronic foot abscess

7. Lymphoid depletion in spleen and thymus

Contributor's Comment: The histochemical stain of a section of brain with Modified Steiner silver stain and immunohistochemical (IHC) stain for *Borrelia burgdorferi* confirmed spiral organisms within areas of inflammation in the meninges of the cerebellum and cerebrum. IHC stains of section of cerebrum for eastern equine encephalitis virus, equine herpes virus-1, West Nile virus, and rabies virus yielded no immunoreactivity. Inflammatory cells were strongly immuno-reactive to CD3 and IBA1; however, rare CD20 and no Pax5 immunoreactivity were detected, confirming lack of plasma cells in areas of inflammation and consistent with common variable immunodeficiency (CVID).

CVID is a primary immunodeficiency disease of humans and horses that encompass a group of heterogenous disorders characterized by hypo-gammaglobulinemia. Generally, at least two isotypes of antibodies are affected, although IgG deficiency alone is recognized. Human CVID patients often present with recurrent respiratory infections and have a high frequency of autoimmune and lympho-proliferative disease.[1,8,9] It is one of the most common primary immuno-deficiencies reported in humans, with an incidence rate of 1 in 25,000 humans. In horses, CVID is a rare condition with relatively few cases reported,[1,2,3,10,14] though the Equine Immunology Laboratory at Cornell College of Veterinary Medicine has diagnosed this condition in over 50 horses since 2002 and has been actively investigating potential genetic and epigenetic mechanisms of disease.[12] Current research on equine CVID focuses on the disruption of B cell development in the bone marrow, and has identified decreased mRNA expression and incomplete demethylation of the *PAX5* gene, required for commitment and differentiation of B cells.[12,13]

Like human patients, horses clinically manifest with recurrent infections of the respiratory tract. In addition, persistent bacterial meningitis has been associated with infection by common skin contaminants such as *Staphylococcus* spp.,[3,10] while *Borrelia burgdorferi* has been highly suspected in other cases of meningitis. One case report of CNS and PNS inflammation in a CVID horse documented a positive Western blot analysis result with low to moderate *Borrelia burgdorferi* antibody response in serum and a positive PCR assay result from CSF using primers for the outer surface protein A (*ospA*) gene.[5] These tests confirm exposure to the bacterium; however, neither test demonstrates active *Borrelia burgdorferi* infection within areas of CNS inflammation. Lyme neuroborreliosis in horses, as with most species, is characterized by suppurative or non-suppurative, lymphoplasmacytic, histiocytic perivascular to diffuse inflammation most severely affecting the CNS, including the meninges, ganglia, and cranial and spinal nerve roots, with varying degrees of necrosis, fibrosis, and neuro-parenchymal invasion.[4]

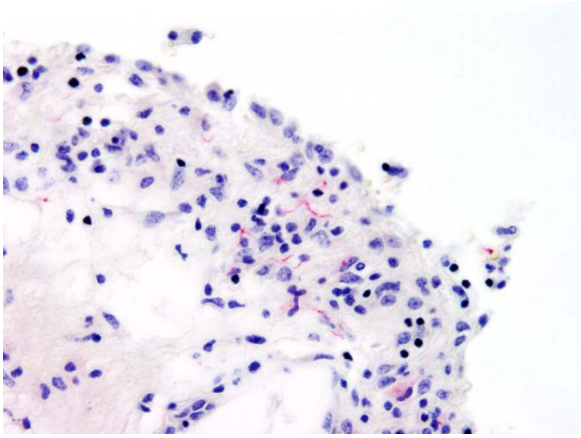

Cerebellar meninges, horse. Immunohistochemical stains demonstrate rare spirochetes perivascular areas within the meninges. (400X).

In the present case, the inflammation is predominately lymphocytic and histiocytic and the distribution includes the spinal cord and ganglia, meninges, choroid plexus, pituitary gland, and neuroparenchyma. By histochemistry and immunohistochemistry, rare spirochetal organisms were present within areas of perivascular inflammation, while a quantitative PCR confirmed the presence of *Borrelia burgdorferi* nucleic acid in the affected cerebrum. The history of uveitis and narcolepsy, the clinical data, histologic findings of severe meningo-myeloencephalitis, choroid plexitis, and hypophysitis, and ancillary testing are consistent with Lyme neuroborreliosis.[4,11] The severe inflammation, fibrosis and parasitic granulomas in the liver, lung, and thymus are attributed to massive parasitic migration; a finding consistent with CVID and a lack of antibody response to parasitic antigens.[2,14] The lack of humoral immunity, the primary host defense mechanism against *Borrelia burgdorferi*, likely contributed to chronic Lyme disease in this horse with CVID.

JPC Diagnosis: Cerebrum: Chorio-meningoencephalitis, lymphohistiocytic, multifocal to coalescing, marked, quarter horse, *Equus ferus caballus.*

Conference Comment: Lyme neuro-borreliosis is an uncommon manifestation of Lyme disease caused by *Borrelia burgdorferi sensu lato* infection in the nervous system, and is typically associated with immunosuppression in horses, humans, and experimental laboratory animal models.[4-6] The contributor provides an outstanding demonstration of that patho-genesis in this case of natural infection in a horse with common variable immuno-deficiency (CVID). As mentioned above, CVID is associated with a late-onset B cell lymphopenia and hypo-gammaglobulinemia with marked decrease in serum IgG. CVID typically manifests as opportunistic recurrent pneumonia, septicemia, and meningitis.[14]

White-footed mice are the principal reservoir host for *B. burgdorferi* in the endemic Northeastern United States, and the bacteria are transferred to susceptible host species by the *Ixodes* sp. tick vector. *B. burgdorferi* localizes in the digestive tract of ixodid ticks via its outer surface protein A (*OspA*) after feeding on an infected reservoir host.[7] When the vector attaches to a susceptible mammalian host and takes a blood meal, there is a subsequent increase in temperature within the tick digestive tract. This change in temperature represses *OspA* expression and induces *OspC* synthesis. This new conformation allows the spirochete to localize to the salivary glands of the tick. Interestingly, this change in conformation can take as long as 48 hours to complete, necessitating the prolonged attachment of the tick to the host. The spirochete then enters the host via the tick's salivary secretions during feeding.[7]

Previous reports of borreliosis in horses have documented arthritis, uveitis, encephalitis, and ataxia.[5] Uveitis, present in this case, is the most common reported extra-neural manifestation of *B. burgdorferi* infection in horses, but is rarely reported in other species.[6] The most common manifestation of disease in dogs is polyarthritis, with fewer cases of membranoproliferative glomerulonephritis.[4-6] Equine neuroborreliosis is challenging to diagnose clinically due to the wide variability in clinical presentation and current lack of reliable antemortem diagnostic tests; however, the conference moderator instructed that the index of suspicion for Lyme disease should be high in horses that present with neurologic deficits and concurrent uveitis.[4-6]

Few conference participants included Lyme disease as a differential diagnosis in this case. Most favored a viral encephalitis caused by an alphavirus (EEE, WEE, VEE), rabies, or West Nile virus due to the relatively non-specific lymphohistiocytic inflammation in this case. Others included equine protozoal myelitis caused by *Sarcocystis neurona*; however, one would expect to see necrotizing granulomatous and eosinophilic lesions, which are not a feature of this case.[6] In conjunction with the excellent images provided by the contributor, the Joint Pathology Center ran a Warthin-Starry silver stain, which highlights numerous argyrophilic spirochetes consistent with *B. burgdorferi* within the inflamed neuroparenchyma. This case demonstrates the importance of including Lyme disease as a differential diagnosis in horses with neurologic disease.

Contributing Institution:
Department of Biomedical Sciences
Section of Anatomic Pathology
College of Veterinary Medicine
Cornell University
Ithaca, NY 14853
http://www.vet.cornell.edu/biosci/pathology/

References:

1. Ardeniz O, Cunningham-Rundles C. Granulomatous disease in common variable immunodeficiency. *Clin Immunol*. 2009; 133:198-201.
2. Flaminio MJBF, LaCombe V, Kohn CW, et al. Common variable immunodeficiency in a horse. *J Am Vet Med Assoc.* 2002; 9:1296-1302.
3. Flaminio MJBF, Tallbridge RL, Salles-Gomes COM, et al. Common variable immunodeficiency in horses is characterized by B cell depletion in primary and secondary lymphoid tissues. *J Clin Immunol.* 2009; 9:107-116.
4. Imai DM, Barr BC, Daft B, et al. Lyme neuroborreliosis in 2 horses. *Vet Pathol*. 2011; 48:1151-1157.
5. James FM, Engiles JB, Beech J. Meningitis, cranial neuritis, and radiculoneuritis associated with *Borrelia burgdorferi* infection in a horse. *J Am Vet Med Assoc.* 2010; 37:1180-1185.
6. Johnstone LK, Engiles JB. Retrospective evaluation of horses diagnosed with neuroborreliosis on postmortem examination: 16 cases (2004-2015). *J Vet Intern Med*. 2016; 30:1305-1312.
7. Kurmaran D, Eswaramoorthy S, et al. Crystal structure of outer surface protein C (OspC) from the lyme disease spirochete, *Borrelia burgdorferi*. *EMBO J*. 2001; 20(5):971-978.
8. Maglione PJ. Autoimmune and lymphoproliferative complications of common variable immunodeficiency. *Curr Allergy Asthma Rep.* 2016; 16:19.
9. Pandit C, Hsu P, van Asperen P, et al. Respiratory manifestations and management in children with common

variable immunodeficiency. *Paediatric Resp Rev.* 2016; Epub ahead of print.
10. Pellegrini-Masini A, Bentz AI, Johns IC, et al. Common variable immunodeficiency in three horses with presumptive bacterial meningitis. *J Am Vet Med Assoc.* 2005; 227:114-122.
11. Priest HL, Irby NL, Schlafer DH, et al. Diagnosis of *Borrelia*-associated uveitis in two horses. *Vet Ophthalmol.* 2012; 15:398-405.
12. Tallmadge RL, Shen L, Tseng CT, et al. Bone marrow transcriptome and epigenome profiles of equine common variable immunodeficiency patients unveil block of B lymphocyte differentiation. *Clin Immunol.* 2015; 160:261-276.
13. Tallmadge RL, Such KA, Miller KC, et al. Expression of essential B cell development genes in horses with common variable immunodeficiency. *Mol Immunol.* 2012; 51:169-176.
14. Tennet-Brown BS, Navas de Solis C, Foreman JH, et al. Common variable immunodeficiency in a horse with chronic peritonitis. *Eq Vet Educ.* 2010; 22:383-399.